Diagnosis of peritonitis using near-infrared optical imaging of *in vivo* labeled monocytes-macrophages

Marcus-René Lisy
Elisabeth Schüler
Friedrich Schiller University Jena
Institute of Diagnostic and Interventional Radiology
FZL Erlanger Allee 101
D-07747 Jena, Germany

Frank Lehmann
Peter Czerney
Dyomics GmbH
Winzerlaer Str. 2A
D-07745 Jena, Germany

Werner A. Kaiser
Ingrid Hilger
Friedrich Schiller University Jena
Institute of Diagnostic and Interventional Radiology
FZL Erlanger Allee 101
D-07747 Jena, Germany

Abstract. Peritonitis is an inflammatory process characterized by massive monocytes-macrophages infiltration. Since early diagnosis is important for a successful therapeutic outcome, the feasibility for a selective labeling and imaging of macrophages for highly sensitive optical imaging was assessed. After *in vitro* incubation of mouse macrophages J774A.1 with the far-red/near-infrared fluorochrome DY-676, distinct fluorescence intensities (1026±142 a.u.) were detected as compared to controls (552±54 a.u.) using a whole-body small animal near-infrared fluorescence (NIRF) imaging system. Macrophage labeling was confirmed by confocal laser scanning microscopy (CLSM) and fluorescence-activated cell sorting, (FACS). The fluorochrome was also found to be predominantly distributed within compartments in the cytoplasm. Additionally, peritonitis was induced in mice by intraperitoneal injection of zymosanA. After intravenous injection of fluorochrome (55 nmol/kg) and using whole-body fluorescence imaging, higher fluorescence intensities (869±151 a.u.) were detected in the peritoneal area of diseased mice as compared to controls (188±41 a.u.). Furthermore, cells isolated from peritoneal lavage revealed the presence of labeled monocytes-macrophages. The results indicate that *in vivo* diagnosis of peritonitis by near-infrared optical imaging of labeled monocytes-macrophages is feasible. Possibly, early stages of other inflammatory diseases could also be detected by the proposed diagnostic method in the long term. [DOI: 10.1117/1.2409310]

Keywords: inflammation; peritonitis; diagnosis; contrast agent; near-infrared fluorescence; optical imaging; inflammation.

Paper 06005R received Jan. 13, 2006; revised manuscript received Aug. 4, 2006; accepted for publication Aug. 10, 2006; published online Jan. 2, 2007.

1 Introduction

Peritonitis is an inflammatory process that can arise from various causes, including infectious, chemical, iatrogenic, and other etiologies. Patients with peritonitis have fever and suffer from abdominal pain and emesis. Various reasons are often described to be responsible for the disease, for instance, the infection of abdominal organs (e.g., the pancreas) or injuries during surgical interventions.[1,2] Even starch or talc from surgical gloves may provoke an abdominal inflammation.[3] In women, peritonitis often occurs after bacterial infection of the uterus.[4] Moreover, patients with kidney failures treated by peritoneal dialysis commonly suffer from this disease.[5]

If untreated, there are many complications resulting from peritonitis that may emerge quite rapidly, such as kidney, lung, and liver failures.[6] Nevertheless, the current diagnostic methods are based on the symptoms and are limited to the application of invasive procedures such as abdominal paracentesis for the assessment of the abdominal fluid in relation to the presence of germs.[7,8] Using radiologic methods, x-ray detections can suggest the presence of the condition, but the diagnostic potential is limited to anatomical information.[9] Occasionally, magnetic resonance tomography (MRT) is used for abdominal imaging and can provide information about inflammatory processes in this cavity. Nevertheless, early detection is not possible by using MRT, particularly because it lacks sensitivity in comparison to other progressive techniques, like positron emission tomography (PET) in nuclear medicine, which is based on radioactive probes as cellular or molecular markers.

At the cellular level, peritonitis, like other inflammatory processes, is characterized by a massive leukocyte infiltration,[10] such as activated monocytes-macrophages into the target tissue 6 to 24 h after onset of inflammation.[11,12] Activation of the monocytes-macrophages population takes place at the highly vascularized internal mucosa layers,[13] where those cells could theoretically be effectively labeled with the aforementioned probes for imaging purposes. The use of far-red and near-infrared fluorescence imaging for the highly sensitive detection of changes on the molecular and cellular level is very attractive. Benefited by the increased capacity of light

Address all correspondence to Dr. Marcus-René Lisy, Friedrich Schiller University of Jena, Institute of Diagnostic and Interventional Radiology, Dept. Experimental Radiology, FZL Erlanger Allee 101, 07747 Jena, Germany. Tel: 0049-3641-9325924; Fax: 0049-3641-9325922; E-mail: Marcus.Lisy@med.uni-jena.de.

1083-3668/2006/11(6)/064014/9/$22.00 © 2006 SPIE

at wavelengths between 600 and 950 nm to penetrate tissues up to a few centimeters,[14,15] fluorochromes, such as indodicarbocyanine (IDCC; $\lambda_{exc.}$: 650 nm; λ_{em}: 670 nm), Cy5.5 (λ_{exc}: 675 nm, λ_{em}: 694 nm) or indocyanine green (ICG, λ_{exc}: 780 nm, λ_{em}: 830 nm) have been used to image specific molecular markers of different diseases.[16–19] In contrast to this, since one of the typical features of macrophages is their phagocytotic activity, it should be possible to simply accumulate fluorochrome in macrophages recruited within inflammatory areas, as this is likely to occur in peritonitis without the need of highly sophisticated contrast agents. Whereas most investigations deal with *ex vivo* labeling using magnetic nanoparticles[20,21] or fluorochromes,[22] *in vivo* fluorochrome tagging of cells has been only poorly considered for imaging until now.[23–25] With the far-red and near-infrared optical methods, a new noninvasive technique has entered the diagnostic field in recent years.[26–28] One particular advantage of this technique is that it can be operated with low costs, easy handling, and without radioactivity.

Therefore, using a novel hemicyanine dye DY-676 (λ_{exc}: 676 nm; λ_{em}: 701 nm) with far-red/near-infrared fluorooptical properties, we addressed the following issues:

- Whether it is possible to label macrophages and to detect them with a whole-body small animal near-infrared imaging system *in vitro* by verifying macroscopic *in vitro* data using flow cytometry and laser scanning microscopy
- Whether it is possible to label monocytes-macrophages *in vivo* in a peritonitis animal model for diagnostic imaging with the whole-body small animal near-infrared fluorescence (NIRF) imaging system.

2 Material and Methods

2.1 *Cell Culture*

Cells from mouse macrophage cell line J774A.1 (Cell Lines Service, Heidelberg, Germany) were cultured in DMEM (Dulbecco Modified Eagle medium; GIBCO BRL, Paisley, Scotland) with 10% (v/v) FCS (fetal calf serum; GIBCO BRL, Paisley, Scotland) at 37 °C in a 5% CO_2 atmosphere and 95% humidity. To label 1.5×10^6 macrophages, cells were incubated for 3 h with the DY-676 (7.7 nmol/ml) or with culture medium only as control for autofluorescence. After washing 10 times with PBS (phosphate buffered saline, 100 mM, pH 7.4) to remove noninternalized dye molecules, cells were scraped from the bottom of the culture dishes and resuspended in PBS for further analysis.

2.2 *In Vitro Far-Red/Near-Infrared Fluorescence Imaging*

Before harvesting, fluorochrome labeled cells were imaged with a planar fluorescence reflectance system, the whole-body small animal near-infrared fluorescence imager (bonSAI, Siemens, Erlangen, Germany), using the 660/735-nm filters for excitation and emission at an acquisition time of 2.0 s with binning factor 2 (512×696 pixels matrix size). Fluorescence signals were detected with a charge-coupled device camera (pixel size 4.6×4.6 μm) and images (regions of interest, ROI) were semiquantitatively analyzed with the SYNGO software (Siemens, Erlangen, Germany). Fluorescence intensities (signal intensities in arbitrary units) were presented as means ± standard deviations. Comparisons of mean fluorescence intensities between labeled and nonlabeled macrophages were performed by means of Students t-test for independent samples.

2.3 *Flow Cytometry Analysis*

In vitro NIRF imaging of macrophages labeled for 24 h with DY-676 was further characterized with a FACSCalibur analytical instrument using the fluorescence channel 3 [FL3, 670-nm long pass (lp)] and the CellQuest software (Becton Dickinson, Heidelberg, Germany). For cell viability testing, cell samples were incubated with 2 μg/ml propidium iodide (Sigma-Aldrich, Steinheim, Germany) for 10 min and fluorescence emission was detected with the fluorescence channel 2 [FL2, 585/42-nm bandpass (bp)].

2.4 *Laser-Scanning Microscopy*

In order to further verify macrophage cell labeling, 10^5 cells incubated with DY-676 (3 h, 7.7 μM) or with culture medium only were additionally sedimented and air-dried on Histobond object slides (Marienfeld, Bad Mergentheim, Germany), stained with 10 μg/ml 4′-6-diamidino-2-phenylindole (DAPI, Sigma-Aldrich, Steinheim, Germany), and embedded with Permafluor (Immunotech, Marseille, France). Confocal laser scanning microscopy was performed using a LSM510 system with the LSM510 image examiner software (Zeiss, Jena, Germany).

2.5 *In Vivo NIRF Imaging of Peritonitis in a Mouse Model*

Nine 8-week-old male NMRI mice weighting approximately 23 g were housed under standard conditions with food and water *ad libitum*. Seven days prior to the start of experiments, all mice received a low pheophorbide diet (Altromin, Lage, Germany) in order to reduce autofluorescence of abdominal organs. At the beginning of the experiments, all animals were shaved on the ventral area. Animals were split into three groups (i), (ii), and (iii), with three animals per group. Peritonitis was induced in mice of groups (i) and (ii) by intraperitoneal injection of 3 mg of zymosanA (Sigma-Aldrich, Steinheim, Germany) dissolved in 400 μl of PBS according to Parente et al.[29] Immediately after induction of peritonitis, mice from group (i) received DY-676 at a dose of 55 nmol of fluorochrome per kg body weight into the tail vein. Group (ii) was not injected with fluorochrome as a control for autofluorescence of macrophages within the target region of diseased mice. Mice from group (iii) got an intraperitoneal injection of 400 μl of PBS (no peritonitis induction) followed by i.v. application of DY-676 as a control for unspecific accumulation of dye in the target region of nondiseased mice. All mice were imaged directly before and at 6 h after (when monocyte-macrophage recruitment starts to increase, as reported by Ajuebor et al.[13]) induction of peritonitis using the whole-body small animal near-infrared fluorescence imaging system, as described earlier. The acquisition time was 0.5 s with binning factor 1 (1024×1392 pixels matrix size). Statistical analysis was performed as described earlier. All procedures were approved by the regional animal committee and were in accordance with international guidelines on the ethical use of animals.

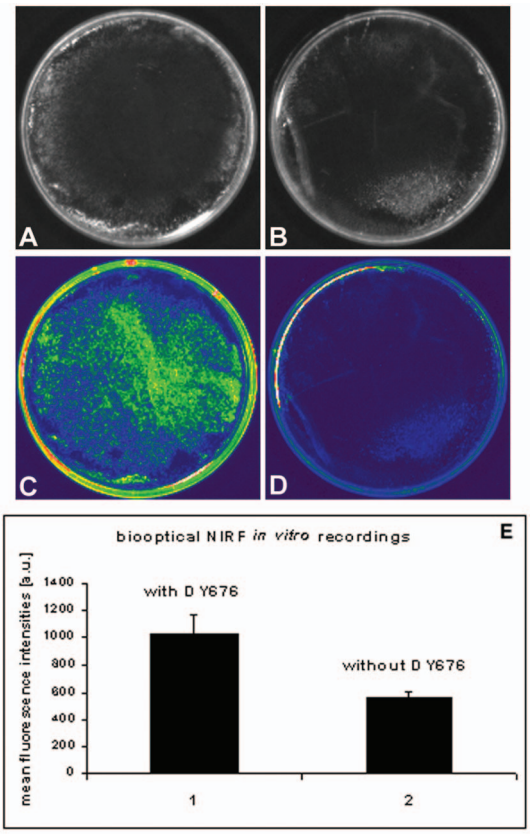

Fig. 1 Biooptical NIRF recordings of *in vitro* labeled J774A.1 macrophages. Macroscopic light [(a) and (b)] and NIRF [(c) and (d), 660/730-nm exc./em] image of petri dishes covered with macrophages after 3 h incubation with DY-676 (7.7 μM in DMEM) [(a) and (c)] or with DMEM medium only [(b) and (d)] (as control for autofluorescence). (e) Semiquantitative ROI-based evaluation of NIRF images with four petri dishes per group: group 1 macrophages incubated with DY-676 (7.7 μM in DMEM), and group 2 macrophages incubated with DMEM only. Data are expressed as means±standard deviations. Differences between group 1 and control group 2 are significant ($P \leq 0.001$).

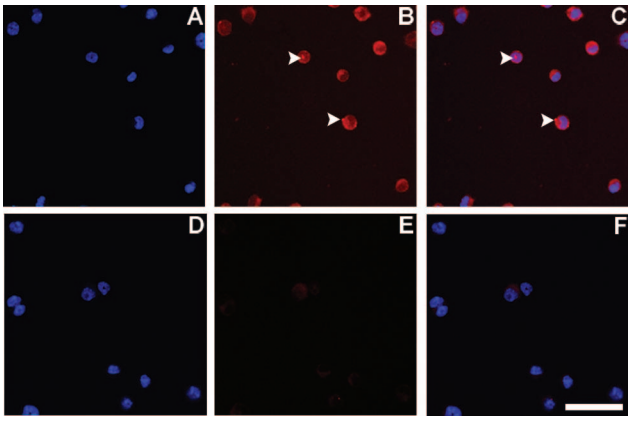

Fig. 2 Localization of DY-676 in *in vitro* labeled J774A.1 macrophages. Upper row: Microscopic (CLSM) image of macrophages incubated for 3 h with DY-676 (7.7 μM in DMEM): (a) DAPI for DNA staining, (b) NIRF (650-nm lp), and (c) merged image. Arrows show endosomal encapsulations of DY-676. Lower row: Macrophages incubated 3 h with DMEM medium only (control for autofluorescence): (d) DAPI for DNA staining, (e) NIRF (650-nm lp), and (f) merged image (scale bar=20 μm).

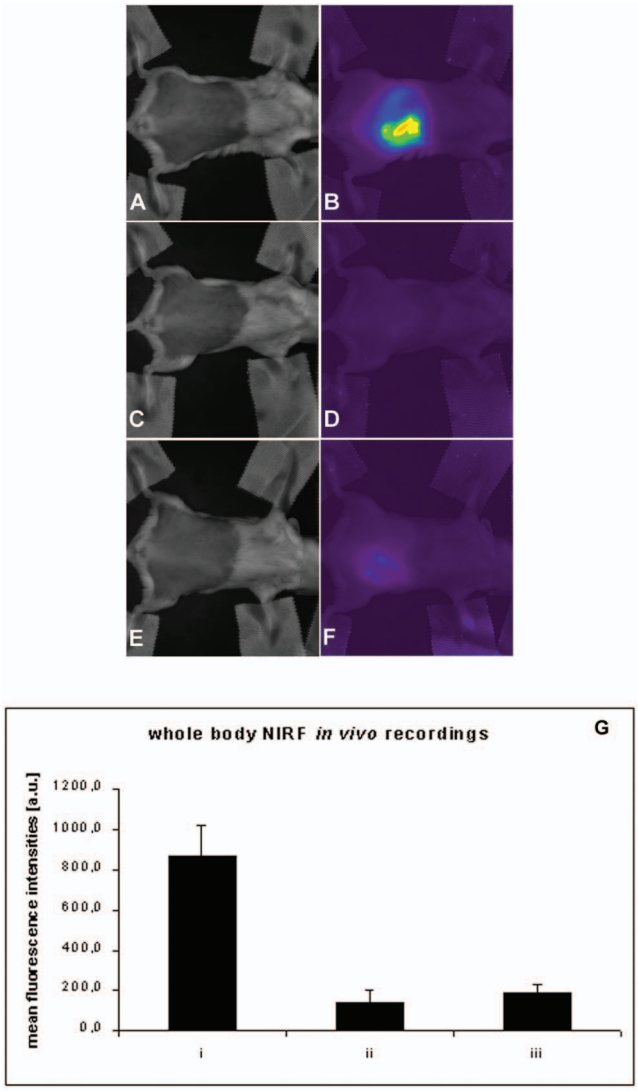

Fig. 4 Whole body NIRF *in vivo* recordings of mice with induced peritonitis. (a) to (f): Macroscopic whole-body images of 8-week-old NMRI mice [left: white light (0.3 s; binning factor 1), right: NIRF, (0.5 s; binning factor 1)]. (a) and (b) Mouse with peritonitis and i.v. application of DY-676 (55 nmol/kg body weight). (c) and (d) Mouse with peritonitis, without DY-676. (e) and (f) Mouse without peritonitis with i.v. application of DY-676 (55 nmol/kg). (g) Semiquantitative ROI-based evaluation of NIRF images with three animals per group: (i) mice with peritonitis and i.v. application of DY-676 (55 nmol/kg), (ii) mice with peritonitis without DY-676, and (iii) mice without peritonitis with i.v. application of DY-676 (55 nmol/kg). Data are expressed as means±standard deviations. Differences between group i and control groups ii and iii are significant ($P \leq 0.01$).

2.6 *Ex Vivo NIRF Imaging of Peritonitis*

6 h after peritonitis induction, the mice were sacrificed and *ex vivo* whole-body NIRF imaging of the opened mice was performed. Afterward, the liver, spleen, and kidneys were withdrawn and imaged as well for assessment of whole-organ fluorescence. The acquisition time was 0.5 s together with a binning factor of 1. Statistical analysis was performed as described earlier. Pieces of the small intestine were snap-frozen, and 6-μm thin sections were immunostained with DAPI and

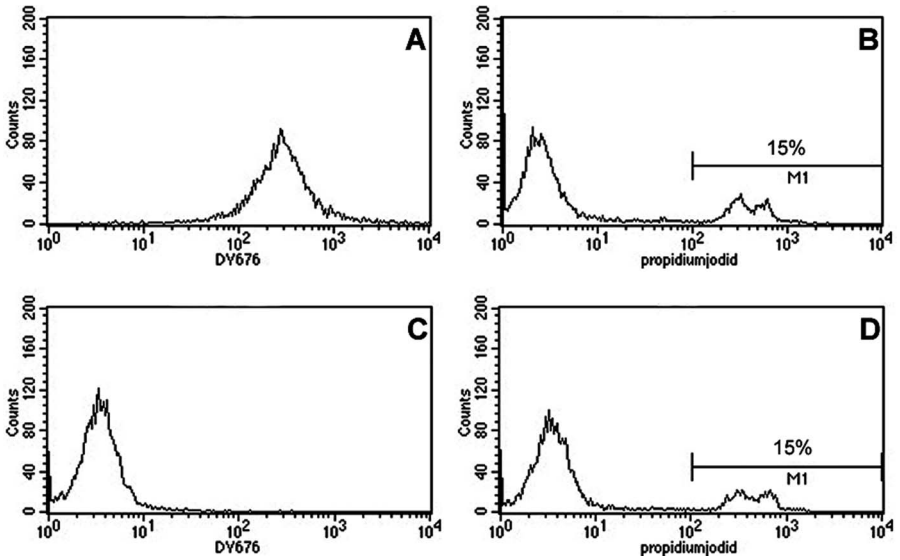

Fig. 3 FACS analysis of *in vitro* labeled J774A.1 macrophages. Histogram blots of macrophages incubated 24 h with 7.7 nmol/ml DY-676 in DMEM [(a) and (b)] or DMEM only (control for autofluorescence) [(c) and (d)]. Images (a) and (c) show relative fluorescence intensities in FL3 channel (670-nm lp); images (b) and (d) show relative fluorescence intensities in FL2 channel (585/42-nm bp) after 10-min propidium iodide incubation for staining of dead cells.

rat anti-mouse CD68 fluoresceinisothiocyanate (FITC)-conjugate (Biozol, Eching, Germany) or rat IgG2a FITC (Serotec, Oxford, UK) as isotype control, respectively, for confocal laser scanning microscopy with the Zeiss LSM510 system.

2.7 *Isolation and NIRF Imaging of Peritoneal Lavage*

In order to verify that *in vivo* NIRF imaging was based on the presence of fluorochrome labeled monocytes-macrophages at the inflamed peritoneal region, all mice received a peritoneal lavage immediately after sacrifice. Hereby, peritoneal cavities were washed with 5 ml of PBS containing 2 mM of ethylenediaminetetraacetic acid (EDTA). The cellular fraction was isolated by centrifugation. In order to assess the presence of fluorochrome labeled cells, pellets containing 5×10^6 cells were imaged with the whole-body small animal near-infrared imaging system as described earlier (acquisition time of 2.0 s and a binning factor of 2). Afterward, cells from peritoneal lavages were then fixated with 3% paraformaldehyde for 15 min followed by careful washing and staining on ice with rat anti-mouse F4/80 FITC conjugate (Dianova, Hamburg, Germany) for 30 min. After extensive washing, cells were analyzed by flow cytometry using the FACSCalibur analytical instrument.

3 Results

3.1 *In Vitro NIRF Imaging of Labeled Macrophages*

Analyses with the whole-body small animal near-infrared fluorescence imaging system showed that fluorochrome labeled macrophages grown on Petri dishes could be clearly identified. After incubation of cells for 3 h with DY-676 (7.7 μM), distinct fluorescence intensities were detected [Fig. 1(a) and 1(c)] as compared to macrophages incubated with medium only [Fig. 1(b) and 1(d)]. Semiquantitative analysis showed significantly increased ($P \leqslant 0.001$) fluorescence intensities of labeled macrophages (1026 ± 142 a.u.) as compared to controls [552 ± 54 a.u., Fig. 1(e)].

The fact that macrophages were, indeed, labeled with the fluorochrome DY-676 was further verified by laser scanning microscopy. It was shown that DY-676 was stored inside the cells. Moreover, no homogeneous distribution inside the cells was observed, but predominantly in compartments with high fluorescence intensity indicating an localized accumulation of fluorochrome (Fig. 2). Flow cytometry analysis revealed that macrophages treated with DY-676 could be clearly distinguished from macrophages that have been incubated with medium only [Fig. 3(a) and 3(c)]. As observed by fluorescence-activated cell sorting (FACS) analysis, more than 99% of all cells in the sample were labeled with the fluorochrome. FACS analysis of propidium-iodide-stained cells revealed that both samples (with and without fluorochrome incubation) contained 85% viable (propidium iodide negative) and 15% nonviable cells (propidium iodide positive) after harvesting [Fig. 3(b) and 3(d)].

3.2 *In Vivo NIRF Imaging of Peritonitis*

Whole-body small animal near-infrared fluorescence imaging showed that 6 h after induction of peritonitis in mice that received the fluorochrome DY-676 [55 nmol/kg, Fig. 4(a) and 4(b)], a distinct fluorescence area was depictable at the left abdominal side, where zymosanA was previously injected. In comparison, control mice without peritonitis (injection of PBS instead of zymosanA) that did receive DY-676 i.v. [Fig. 4(e) and 4(f)] showed a spot at the abdominal area with a comparatively much lower fluorescence intensity. Nevertheless, mice having peritonitis that did not receive the contrast medium DY-676 [control for autofluorescence of monocytes-macrophages within the target region of diseased mice, Fig. 4(c) and 4(d)] revealed no fluorescence at all. Semiquantita-

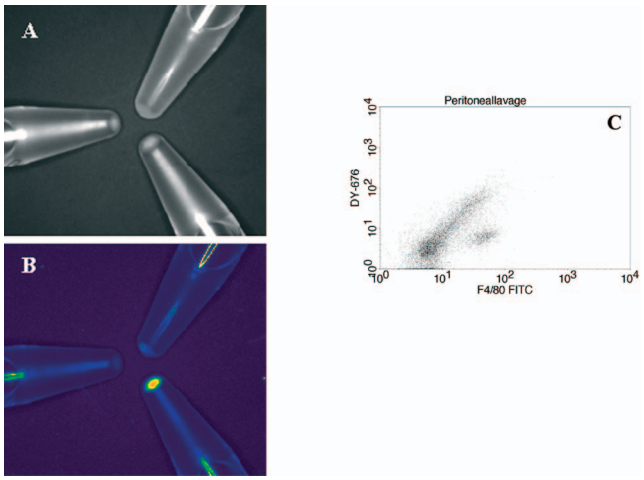

Fig. 5 *Ex vivo* NIRF imaging of macrophages from mice with and without peritonitis. (a) White-light image (0.3 s, binning factor 2) and (b) NIRF image (2.0 s; binning factor 2) of cell pellets from peritoneal lavage from 8-week-old NMRI mice. Lower-right sample: cells from mouse with peritonitis with i.v. application of DY-676 (55 nmol/kg). Upper-right sample: cells from mouse without peritonitis with i.v. application of DY-676 (55 nmol/kg, control for unspecific dye accumulation). Left sample: cells from mouse with peritonitis without i.v. application of DY-676 (control for autofluorescence). (c) Flow cytometric analysis of the cellular peritoneal infiltrate. The peritoneal lavages of mice from group i were incubated with F4/80 FITC conjugated mAb before FACS analysis. DotBlot shows relative fluorescence intensities in FL3 channel (670-nm lp, DY-676) and relative fluorescence intensities in FL1 channel (530/30-nm, bp, F4/80).

tive analysis of mice abdominal areas showed that 6 h after induction of peritonitis, fluorescence intensities of the ventral areas with peritonitis [group (i), 869±87 a.u.] were increased by a factor of 4 or higher compared to the data of both control groups (ii) (142±35 a.u.) and (iii) [188±24 a.u., Fig. 4(g)].

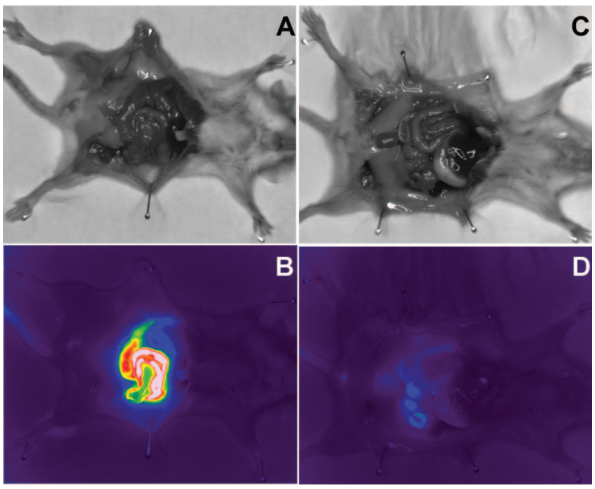

Fig. 6 Whole-body NIRF *ex vivo* recordings of mice with induced peritonitis. Macroscopic images [white light above (0.3 s; binning factor 1) and NIRF below (0.5 s; binning factor 1)] of sacrificed 8-week-old NMRI mice 6 h after i.v. injection of DY-676 (55 nmol/kg). (a) and (b) mouse with peritonitis, and (c) and (d) mouse without peritonitis (control for selective macrophage labeling).

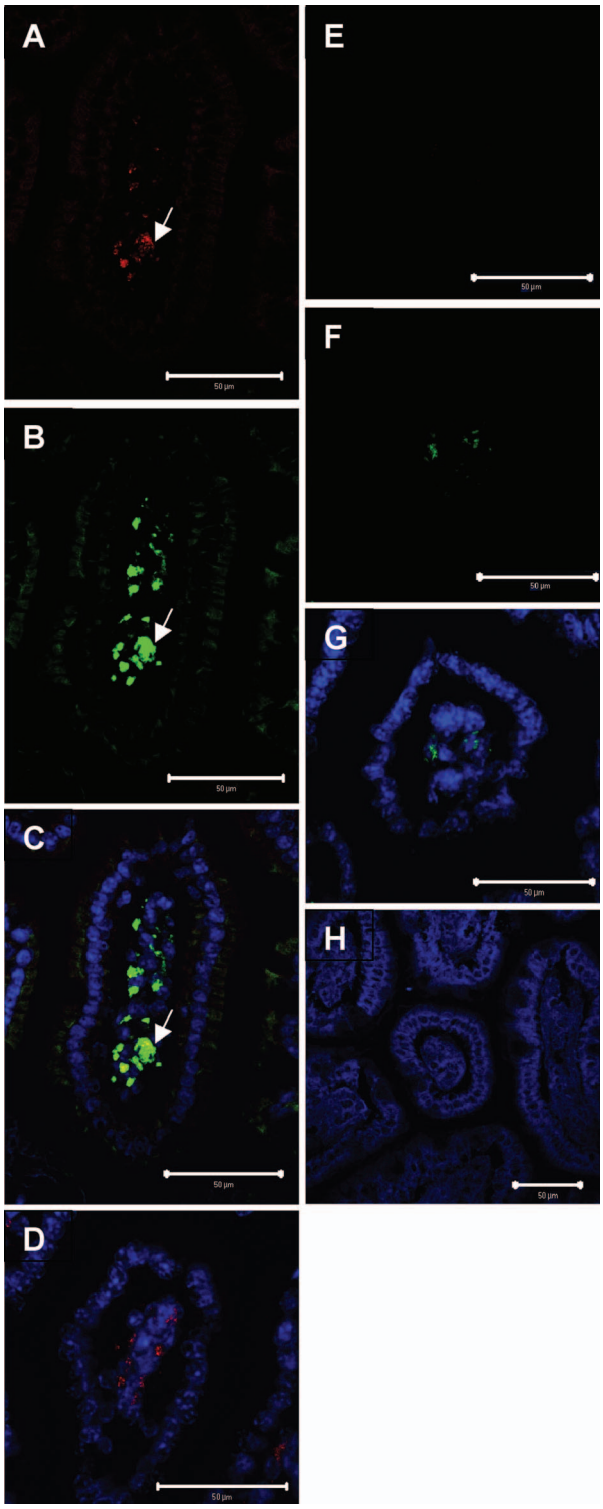

Fig. 7 Immunofluorescence staining of the small intestine of diseased mice. (a) NIRF (red, >650-nm lp), (b) CD68FITC, (c) merged with DAPI for DNA staining (blue), and (d) rat IgG2a FITC isotype control (green) images derived from a mouse 6 h after injection of DY-676. Arrows show $CD68^+$ monocytes-macrophages located in the lamina propria of villi within the mucosa containing DY-676. Images (e) NIRF (red, >650-nm lp), (f) CD68FITC (green), (g) merged with DAPI for DNA staining (blue), and (h) rat IgG2a FITC isotype control (green) images derived from a diseased mouse without injection of DY-676 (scale bars=50 μm).

3.3 *Ex Vivo NIRF Imaging of Peritoneal Lavage from Mice with and without Peritonitis*

Analysis of cells isolated from peritoneal lavage using the whole-body small animal near-infrared imaging system [Fig. 5(a) and 5(b)] showing reaction cups containing cell sediments) revealed the presence of fluorochrome labeled cells only in samples from mice with peritonitis having received the contrast agent DY-676 [high fluorescence in the lower-right reaction cup, Fig. 5(b)]. In contrast, isolated cells from peritoneal lavage of mice with peritonitis but without contrast agent [left reaction cup, Fig. 5(b)] showed no fluorescence intensity. The cell sediment in the upper-right reaction cup derived from mice that were only injected i.v. with DY-676 but without induction of peritonitis revealed very weak signal intensities [Fig. 5(b)].

For the assessment of the constitution of the fraction of fluorescent cells in the peritoneal lavage collected from mice of group (i), the rat anti-mouse F4/80 FITC conjugate was used as a marker for tissue macrophages. Flow cytometric analysis revealed the presence of distinct populations on the basis of forward and side scatter profiles (data not shown) as well as on the basis of fluorescence emission [Fig. 5(c)]. The DotBlot clearly shows that cells with intermediate and high expression levels of F4/80 antigen (28%) also revealed fluorescence intensities in the far-red/near-infrared range, whereas F4/80 negative cells (61%) did not. A third fraction of F4/80 positive cells (11%) revealed no fluorescence in the far-red/near-infrared range.

3.4 *Ex Vivo NIRF Imaging of Mice with and without Peritonitis*

The whole-body NIRF images of opened mice with peritonitis having received an i.v. injection of DY-676 showed areas of distinctly higher fluorescence intensities on the surface of the intestinal tract [Fig. 6(a) and 6(b)] as compared to mice without peritonitis but with i.v. injection of DY-676 [Fig. 6(c) and 6(d)].

Immunostaining of the small intestine from diseased mice that were injected with DY-676 clearly showed that CD68-positive monocytes-macrophages located in the lamina propria of villi within the mucosa revealed high fluorescence intensities in the far-red/near-infrared range [Fig. 7(a)–7(c)]. Moreover, CD68-positive monocytes-macrophages between the crypts were found to be intracellularly loaded with DY-676 (data not shown). Whereas no fluorescence was observed using the FITC-labeled isotype control, far-red/near-infrared fluorescent spots were still detected within the centers of the lamina propria [Fig. 7(d)]. Immunostaining of the small intestine from diseased mice without injection of DY-676 showed no fluorescence intensities in the far-red/near-infrared range [Fig. 7(e)–7(h)].

Whole-organ fluorescence analysis [Fig. 8(a)–8(f)] showed that some signal was detectable in the kidneys from mice both with and without peritonitis after application of the contrast medium DY-676 [Fig. 8(d) and 8(f)]. In comparison no fluorescence was observed in mice having received no DY-676 [Fig. 8(d)]. Semiquantitative analysis supported the aforementioned findings [Fig. 8(g)]. Particularly, low mean fluorescence intensities of 210 to 270 a.u. were detected in the kidneys of mice intravenously injected with DY-676, whereas the mean fluorescence intensities of all other organs were even lower than 100 a.u.

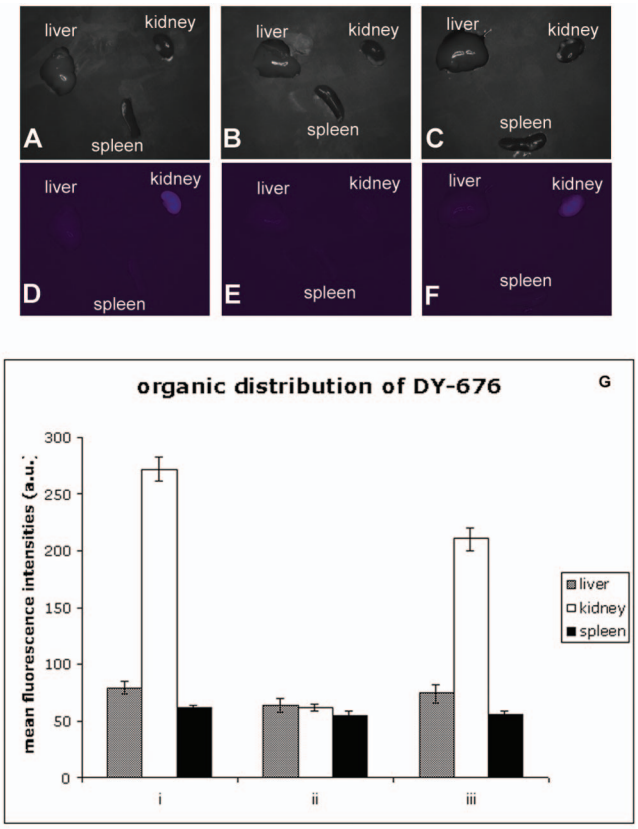

Fig. 8 Biooptical NIRF *ex vivo* recordings of organs from mice with induced peritonitis. Macroscopic images [white light, above (0.3 s, binning factor 1) and NIRF below (0.5 s, binning factor 1)] of withdrawn organs from mouse with both peritonitis and i.v. application of DY-676 (55 nmol/kg) [(a) and (d)]; mouse with peritonitis without i.v. application of DY-676 [(b) and (e)]; and mouse without peritonitis with i.v. application of DY-676 (55 nmol/kg) [(c) and (f)]. (g) Semiquantitative ROI-based evaluation of NIRF images with three animals per group: (i) mice with peritonitis and i.v. application of DY-676 (55 nmol/kg), (ii) mice with peritonitis without DY-676, and (iii) mice without peritonitis with i.v. application of DY-676 (55 nmol/kg). Data are expressed as means±standard deviations.

4 Discussion

Our results revealed that monocytes-macrophages could be efficiently labeled with DY-676 and imaged *in vitro* and *in vivo* using a whole-body near-infrared fluorescence imaging system.

The *in vitro* experiments with mouse macrophage cell line J774A.1 showed that cells could be selectively imaged with a whole-body small animal imaging system after labeling with DY-676. Macrophage labeling with DY-676 was clearly verified by FACS analysis; however, as compared to the aforementioned results, semiquantitative analysis of the images obtained from the whole-body small animal imaging system showed relatively higher fluorescence intensities of nonlabeled cells in relation to the labeled ones. These findings can be attributed to the reflective effects of the culture dishes' smooth surface. Further on, FACS analysis using propidium

iodide revealed that incubation with fluorochrome for 24 h does not affect cell viability. The histogram blots showed that there were only 15% of death cells both in DY-676 labeled and in nonlabeled samples. The presence of dead cells was probably caused by scraping off from the plastic matrix. With respect to the *in vivo* situation, this observation basically indicates that labeling of macrophages with fluorochromes should not have an impact on cell viability. Moreover, DY-676 was predominantly stored within defined structures of the cytoplasm, which is presumably caused by the active uptake into organelles like endosomes during phagocytosis. The exact mechanisms for uptake of fluorochromes in macrophages are not clear yet. Nevertheless, active phagocytosis of dyes after binding to serum albumin has been already discussed[24] in relation to the application of Cy5.5. Since the chemical structure of DY-676 is similar to that of Cy 5.5, it is conceivable that some unspecific binding of the dye to serum proteins takes place. In this case, dye uptake by macrophages occurs via phagocytosis.

In vivo whole-body fluorescence imaging of mice at 6 h after zymosanA-induced peritonitis showed that mice suffering from this disease could be clearly distinguished from controls, indicating that, basically, an early specific identification of the disease is possible using optical methods. Due to the fact that clearance of the fluorochrome in healthy mice takes between 4 and 6 h and as we intended to demonstrate feasibility to image early stages of inflammation, when monocytes-macrophages start to migrate to the target area, it was necessary to inject the contrast agent immediately after induction of peritonitis. Other studies reported that monocyte-macrophage infiltration takes place for more than 24 h.[11,13] Therefore, peritonitis could also be detected at later points in time, which has to be proven in further studies. Considering the clinical situation, a very effective monitoring of patients, e.g., during surgery, could be performed when monocytes-macrophages start to migrate to the target area, but further studies are necessary to elucidate to what extent the characteristics of the peritonitis model used in the present study are transferable to human beings.

All fluorescence data shown in the present study are based on semiquantitative analysis of intrinsic values of the CCD camera calculated by the SYNGO software. The influence of inhomogeneous absorptive behaviour, reflection, or scattering properties[30] of the samples or tissues investigated in this study could not be considered. Nevertheless, as equivalent experimental conditions were used, the interpretation of semiquantitative data is legitimate to show tendencies. The observed differences between the contrast in *in vitro* and *in vivo* experiments are not clear, but it is conceivable that the unspecific reflections in relation to the Petri dishes used in the present study in the *in vitro* situation may have influenced the results.

The aforementioned *in vivo* observations are in agreement with the results from *ex vivo* examinations showing that the application of the contrast medium led to a selective labeling of macrophages recruited at the target site. These results are reinforced, in principle, by the fact that the animal model used is known to be characterized by a massive recruitment of activated monocytes-macrophages into the peritoneum at the area of zymosanA injection, which increases between 6 h and 24 h after induction of peritonitis.[13] Presumably, *in vivo* uptake of DY-676 by monocytes-macrophages occurs in well vascularized mucosa layers before immigration into the inflamed region takes place. This assumption is reinforced by the observations of Ajuebor et al.,[13] who reported a pronounced migration of monocytes-macrophages from the peritoneum to the internal mucosa layers followed by a reappearence at the area of zymosanA injection. Further studies should consider and verify these relationships in more detail as well as identify to what extent they apply in connection with the situation in humans.

The presence of fluorochrome labeled cells in peritoneal lavages extracted from the inflamed region could be confirmed by analysis of NIRF images of cell sediments. In particular, the strong fluorescence of the cell sediments derived from the diseased mice after i.v. DY-676 application corresponds well to the *in vivo* results. The weak signal of the isolated cells from the mice without peritonitis that received only contrast agent might be caused by the presence of labeled monocytes-macrophages in consequence of the intervention itself, as demonstrated by the injection of harmless PBS instead of zymosanA. As expected from the *in vivo* results, no fluorescent cells could be found in cells from diseased mice that were not injected with the DY-676, indicating that autofluorescence emerging from monocytes-macrophages *per se* or zymosanA itself had no effects on the observed fluorescence signals.

The fact that *in vivo* the fluorochrome DY-676 was mainly taken up by monocytes-macrophages was demonstrated by FACS analysis. Hereby, cells expressing intermediate and high levels of F4/80 antigen were found to show fluorescence intensities in the far-red/near-infrared range. Moreover, these results are consistent with previous reports[13,31] showing that the F4/80 antigen is expressed on monocytes-macrophages reappearing very early at the area of zymosanA injection up to 24 h after onset of peritonitis. Further on, it was reported that after immunostaining of cells from peritoneal lavages against the F4/80 antigen, three subpopulations (lymphocytes—non-expressing; monocytes—intermediate levels; and macrophages—high levels) were identified.[13] In accordance with that study, we state that monocytes-macrophages could be identified as the fraction of cells in the peritoneal lavage collected containing the contrast agent DY-676. Moreover, the fact that *in vivo* whole-body fluorescence signals are based on fluorochrome labeled monocyte-macrophages is further reinforced by immunofluorescence analysis of the small intestine from the area of zymosanA injection.

Whereas the results indicate that the detected fluorescence signals are mainly associated with labeled cells, a nonspecific accumulation of fluorochrome at the target region seems to be unlikely because controls injected with PBS only instead of the zymosanA suspension showed only very weak fluorescence *in vivo* at the target site. This is supported by the *ex vivo* images of opened control mice, where only very low fluorescence intensities could be detected on the surface of the intestinal tract, due to the lack of an increased monocyte-macrophage population.

Compared to the fluorescence signals observed in the peritoneal area of zymosanA injection, only very low signals were detectable in the withdrawn highly vascularized organs, like the kidneys, liver, and spleen. Particularly for the kidneys, the determined "out of body" fluorescence values are lower by a

factor of 3 in comparison to the results from the *in vivo* images. Moreover, *in vivo* whole-body imaging of mice without peritonitis injected with DY-676 revealed no detectable fluorescence in the liver and kidneys. Therefore, the low signal intensities in these vascularized organs should not have contributed to the observed fluorescence intensity at the inflamed abdominal region.

The very low signals emitted from the kidneys suggest a fast renal clearance mechanism of the fluorochrome that would be an advantage in relation to those macromolecular contrast agents with a predominant hepatic deposition and metabolism, like the clinically used indocyanine green[32] or the previously reported high-affinity contrast agents, where fluorochrome molecules (e.g., Cy5.5) were coupled to macromolecular antibodies (e.g., Herceptin) for tumor imaging.[23,33] This is, to the best of our knowledge, the first time that peritoneal macrophages have been efficiently labeled and imaged using fluorochrome dyes.

Whereas the results of the present study indicate that peritonitis could be selectively detected by optical methods, one of the possible limitations of this method consists of the lack of an adequate anatomical resolution that is associated with the optical systems available up to now. The *in vivo* findings presented here are based on planar fluorescence reflectance imaging. No real tomographic information for exactly three-dimensional resolution of the inflammatory areas was available. Nevertheless, different techniques like the very interesting approaches[34] related to fluorescence mediated tomography (FMT) or the combination of NIRF imaging with other tomographic devices should be valuable tools for providing further detailed information about the respective inflammatory region.

The present study shows that monocyte-macrophage cultures can be successfully labeled and imaged in their original size using a fluoro-optical contrast medium and that, accordingly, selective macrophage labeling and whole-body imaging could also be performed in the *in vivo* situation, particularly in relation to the detection of peritonitis as demonstrated in an animal model. Furthermore, labeling of monocytes-macrophages with DY-676, as shown in the present study, as well as using other potentially nontoxic NIRF fluorochromes, can be suitable for clinical diagnostics of other inflammatory diseases. In that case, this technology would be limited to diseases that are located only a few centimeters below the skin, due to the limited penetration depth of far-red/near-infrared light. In our study, we intended to show the basic feasibility using planar optical imaging whereby light penetration into tissue is limited. However, based on the fact that peritonitis is localized only a few cm under the skin surface, it is conceivable that peritonitis in humans could be detected with fluorescence-mediated tomography (penetration depth >10 cm; Ref. 34). For more detailed *in vivo* imaging of developing inflammatory processes, additional studies should focus on specific target molecules such as cytokines and their receptors.

Acknowledgments

The authors would like to thank Dr. Harald Schubert (Institute for Animal Research, University of Jena, Germany), Yvonne Heyne, and Brigitte Maron for excellent technical assistance.

References

1. J. I. Greenfeld and C. M. Harmon, "Acute pancreatitis," *Curr. Opin. Pediatr.* **9**, 260–264 (1997).
2. H. B. Reith, "Therapy of peritonitis today: surgical management and adjuvant therapy strategies," *Langenbecks Arch. Chir.* **382**, S14–S17 (1997).
3. H. Ellis, "The hazards of surgical glove dusting powders," *Surg. Gynecol. Obstet.* **171**, 521–527 (1990).
4. J. Paavonen, "Pelvic inflammatory disease: from diagnosis to prevention," *Dermatol. Clin.* **16**, 747–756 xii (1998).
5. R. W. Steiner and N. A. Halasz, "Abdominal catastrophes and other unusual events in continuous ambulatory peritoneal dialysis patients," *Am. J. Kidney Dis.* **15**, 1–7 (1990).
6. H. Wacha, T. Hau, R. Dittmer, and C. Ohmann, "Risk factors associated with intraabdominal infections: a prospective multicenter study: Peritonitis Study Group," *Langenbecks Arch. Chir.* **384**, 24–32 (1999).
7. V. Golash and P. D. Willson, "Early laparoscopy as a routine procedure in the management of acute abdominal pain: a review of 1,320 patients," *Surg. Endosc* **19**, 882–885 (2005), epub 12 May 2005.
8. A. Farooq and B. J. Ammori, "Laparoscopic diagnosis and management of primary bacterial peritonitis," *Surg. Laparosc. Endosc. Percutan. Tech.* **15**, 36–37 (2005).
9. A. Korzets, Z. Korzets, G. Peer, J. Papo, D. Stern, J. Bernheim, and M. Blum, "Sclerosing peritonitis: possible early diagnosis by computerized tomography of the abdomen," *Am. J. Nephrol.* **8**, 143–146 (1988).
10. C. J. van der Laken, O. C. Boerman, W. J. Oyen, P. Laverman, M. T. van de Ven, F. H. Corstens, and J. W. van der Meer, "*In vivo* expression of interleukin-1 receptors during various experimentally induced inflammatory conditions," *J. Infect. Dis.* **177**, 1398–1401 (1998).
11. S. J. Getting, R. J. Flower, L. Parente, R. de Medicis, A. Lussier, B. A. Woliztky, M. A. Martins, and M. Perretti, "Molecular determinants of monosodium urate crystal-induced murine peritonitis: a role for endogenous mast cells and a distinct requirement for endothelial-derived selectins," *J. Pharmacol. Exp. Ther.* **283**, 123–130 (1997).
12. R. W. Kinne, R. Brauer, B. Stuhlmuller, E. Palombo-Kinne, and G. R. Burmester, "Macrophages in rheumatoid arthritis," *Arthritis Res.* **2**, 189–202 (2000).
13. M. N. Ajuebor, R. J. Flower, R. Hannon, M. Christie, K. Bowers, A. Verity, and M. Perretti, "Endogenous monocyte chemoattractant protein-1 recruits monocytes in the zymosan peritonitis model," *J. Leukoc Biol.* **63**, 108–116 (1998).
14. K. Konig, "Multiphoton microscopy in life sciences," *J. Microsc.* **200**, 83–104 (2000).
15. Z. Gryczynski, I. Gryczynski, and J. R. Lakowicz, "Fluorescence-sensing methods," *Methods Enzymol.* **360**, 44–75 (2003).
16. A. Becker, C. Hessenius, K. Licha, B. Ebert, U. Sukowski, W. Semmler, B. Wiedenmann, and C. Grotzinger, "Receptor-targeted optical imaging of tumors with near-infrared fluorescent ligands," *Nat. Biotechnol.* **19**, 327–331 (2001).
17. K. Licha, C. Hessenius, A. Becker, P. Henklein, M. Bauer, S. Wisniewski, B. Wiedenmann, and W. Semmler, "Synthesis, characterization, and biological properties of cyanine-labeled somatostatin analogues as receptor-targeted fluorescent probes," *Bioconjugate Chem.* **12**, 44–50 (2001).
18. R. Weissleder and U. Mahmood, "Molecular imaging," *Radiology* **219**, 316–333 (2001).
19. K. Licha, B. Riefke, V. Ntziachristos, A. Becker, B. Chance, and W. Semmler, "Hydrophilic cyanine dyes as contrast agents for near-infrared tumor imaging: synthesis, photophysical properties and spectroscopic *in vivo* characterization," *Photochem. Photobiol.* **72**, 392–398 (2000).
20. M. Lewin, N. Carlesso, C. H. Tung, X. W. Tang, D. Cory, D. T. Scadden, and R. Weissleder, "Tat peptide-derivatized magnetic nanoparticles allow *in vivo* tracking and recovery of progenitor cells," *Nat. Biotechnol.* **18**, 410–414 (2000).
21. U. Himmelreich, R. Weber, P. Ramos-Cabrer, S. Wegener, K. Kandal, E. M. Shapiro, A. P. Koretsky, and M. Hoehn, "Improved stem cell MR detectability in animal models by modification of the inhalation gas," *Mol. Imaging* **4**, 104–109 (2005).
22. R. W. Dirks, C. Molenaar, and H. J. Tanke, "Visualizing RNA molecules inside the nucleus of living cells," *Methods* **29**, 51–57 (2003).

23. B. Ballou, G. W. Fisher, A. S. Waggoner, D. L. Farkas, J. M. Reiland, R. Jaffe, R. B. Mujumdar, S. R. Mujumdar, and T. R. Hakala, "Tumor labeling *in vivo* using cyanine-conjugated monoclonal antibodies," *Cancer Immunol. Immunother* **41**, 257–263 (1995).
24. A. Hansch, O. Frey, I. Hilger, D. Sauner, M. Haas, D. Schmidt, C. Kurrat, M. Gajda, A. Malich, R. Brauer, and W. A. Kaiser, "Diagnosis of arthritis using near-infrared fluorochrome Cy5.5," *Invest. Radiol.* **39**, 626–632 (2004).
25. X. Dong, S. Swaminathan, L. A. Bachman, A. J. Croatt, K. A. Nath, and M. D. Griffin, "Antigen presentation by dendritic cells in renal lymph nodes is linked to systemic and local injury to the kidney," *Kidney Int.* **68**, 1096–1108 (2005).
26. R. R. Alfano, S. G. Demos, and S. K. Gayen, "Advances in optical imaging of biomedical media," *Ann. N.Y. Acad. Sci.* **820**, 248–271 (1997).
27. S. Andersson-Engels, C. Klinteberg, K. Svanberg, and S. Svanberg, "*In vivo* fluorescence imaging for tissue diagnostics," *Phys. Med. Biol.* **42**, 815–824 (1997).
28. J. C. Hebden and D. T. Delpy, "Diagnostic imaging with light," *Br. J. Radiol.* **70**, S206–S214 (1997).
29. M. Perretti, E. Solito, and L. Parente, "Evidence that endogenous interleukin-1 is involved in leukocyte migration in acute experimental inflammation in rats and mice," *Agents Actions* **35**, 71–78 (1992).
30. V. Ntziachristos, J. Ripoll, L. V. Wang, and R. Weissleder, "Looking and listening to light: the evolution of whole-body photonic imaging," *Nat. Biotechnol.* **23**, 313–320 (2005).
31. J. F. Cailhier, M. Partolina, S. Vuthoori, S. Wu, K. Ko, S. Watson, J. Savill, J. Hughes, and R. A. Lang, "Conditional macrophage ablation demonstrates that resident macrophages initiate acute peritoneal inflammation," *J. Immunol.* **174**, 2336–2342 (2005).
32. S. G. Ketterer, B. D. Wiegand, and E. Rapaport, "Hepatic uptake and biliary excretion of indocyanine green and its use in estimation of hepatic blood flow in dogs," *Am. J. Physiol.* **199**, 481–484 (1960).
33. I. Hilger, Y. Leistner, A. Berndt, C. Fritsche, K. M. Haas, H. Kosmehl, and W. A. Kaiser, "Near-infrared fluorescence imaging of HER-2 protein over-expression in tumour cells," *Eur. Radiol.* **14**, 1124–1129 (2004).
34. V. Ntziachristos, C. Bremer, and R. Weissleder, "Fluorescence imaging with near-infrared light: new technological advances that enable *in vivo* molecular imaging," *Eur. Radiol.* **13**, 195–208 (2003).